Journal of *Marine Science and Engineering*

MDPI

Article

CO_2 Injection Monitoring: Enhancing Time-Lapse Seismic Inversion for Injected Volume Estimation in the Utsira Formation, Sleipner Field, North Sea

Doyin Pelemo-Daniels *, Basil O. Nwafor * and Robert R. Stewart *

Department of Earth and Atmospheric Sciences, University of Houston, Science and Research Building 1, 3507 Cullen Blvd, Room 312, Houston, TX 77204-5007, USA

* Correspondence: oooyetu2@cougarnet.uh.edu (D.P.-D.); bonwafor@cougarnet.uh.edu (B.O.N.); rrstewart@uh.edu (R.R.S.)

Abstract: This article presents an in-depth study of CO_2 injection monitoring in the Sleipner Field, focusing on the Utsira Formation. The research leverages advanced time-lapse inversion techniques and 4D seismic data analysis to enhance the accuracy of volume estimations and provide a comprehensive understanding of the dynamic behavior of the injected CO_2 plume. The analysis encompasses cross correlation, time shift, predictability, and other key elements to yield robust insights into the reservoir's response to CO_2 injection. Cross-correlation analysis results of 60% to 100% outside the injection zone and less than 50% within the injection zone reveal a distinct dissimilarity between the injection and non-injection zones, emphasizing phase, time, and frequency content changes due to CO_2 injection. Time shifts are meticulously calibrated globally on a trace-by-trace basis, to account for shallow statics and velocity changes, improving the overall alignment of seismic data. Predictability analysis results of 0 to 0.34 within the injection zone and 0.45 to 0.96 at the background further reinforce the findings, highlighting high predictability values in areas untouched by production and markedly lower values within the injection zone. These results provide a measure of the reliability of the seismic data and its ability to reflect the subtle changes occurring in the reservoir. Crucially, the time-lapse inversion process excels in capturing the evolving state of the CO_2 plume within the Utsira Formation. The seismic data reveals the migration and expansion of the plume over time and the dynamic nature of the reservoir's response to CO_2 injection. Integrating various data facets reduces non-uniqueness in inversion results, allowing for more precise volume estimations.

Keywords: Sleipner; time-lapse inversion; CO_2 monitoring; seismic interpretation; carbon capture; CCUS; CCS

Citation: Pelemo-Daniels, D.; Nwafor, B.O.; Stewart, R.R. CO_2 Injection Monitoring: Enhancing Time-Lapse Seismic Inversion for Injected Volume Estimation in the Utsira Formation, Sleipner Field, North Sea. *J. Mar. Sci. Eng.* **2023**, *11*, 2275. https://doi.org/10.3390/jmse11122275

Academic Editor: George Kontakiotis

Received: 23 October 2023
Revised: 14 November 2023
Accepted: 15 November 2023
Published: 30 November 2023

1. Introduction

The global challenge of mitigating greenhouse gas (GHG) emissions and addressing climate change has led to the adoption of innovative technologies like carbon capture, utilization, and storage (CCUS) [1]. CCUS holds significant promise for reducing CO_2 emissions from industrial sources and power plants by capturing and securely storing CO_2 underground. As CCUS projects scale up, robust and continuous monitoring of injected CO_2 within subsurface reservoirs becomes crucial to ensure the process's effectiveness and safety [2].

The immediate effects of CO_2 injection, including monitoring migration patterns, pressure changes, and geo-mechanical responses within the reservoir has generated more interest [3,4]. However, a critical aspect often overlooked in these studies is the long-term consequence and behavior of the injected CO_2 over time. The central question arising from this knowledge gap is whether the volume of CO_2 injected remains equivalent to the amount of CO_2 in the reservoir over extended periods [5]. This question is relevant from an environmental perspective and carries profound implications for the effectiveness and

safety of CCUS projects. Ensuring that the injected CO_2 does not leak into the atmosphere or migrate to unintended areas within the subsurface formations is crucial [5,6].

Time-lapse inversion techniques offer a unique advantage in estimating CO_2 volume and plume advancement compared to other methods such as gravity measurements, observation wells, due to their ability to provide dynamic, high-resolution imaging of subsurface changes over time [7]. For instance, while gravity measurements provide indirect information on subsurface changes, they might lack the spatial resolution and specificity to precisely track CO_2 plume advancement. By combining data from observation wells with time-lapse inversion, it is possible to validate and refine the spatial distribution of the plume. This integration can enhance the accuracy and coverage of the plume's advancement assessment. Integrating these methods to corroborate findings increases the overall accuracy and understanding of CO_2 plume behavior [8,9]. In this research, we integrated data from an observation well with time-lapse inversion. This helps to validate and refine the spatial distribution of the plume and enhances the accuracy and coverage of the plume's advancement assessment.

The effectiveness of time-lapse inversion is heavily influenced by the quality and resolution of seismic data and the calibration parameters used [10]. High-quality seismic data enhances the precision of the technique, offering clearer images of subsurface changes. Calibration parameters determine the accuracy of the model used in the inversion process. If these parameters are not well calibrated, the results will not reflect the actual changes in CO_2 distribution accurately [10–12]. In this research. We enhanced our time-lapse inversion result by ensuring accurate calibration parameters to avoid skewing the results and misrepresenting the plume's behavior.

Several authors [13,14] have tried to estimate the thickness and velocity changes of injected CO_2 layers from prestack time-lapse seismic data using amplitude and time-shift analysis. Furthermore, time-lapse 3D seismic surveys were employed to evaluate the efficacy of these methods in providing consistent and comprehensive three-dimensional spatial monitoring of the storage complex [15]. Also, their study aimed to establish a quantitative tool for detecting potential leakage. Nevertheless, it is worth noting that a limited amount of research and analysis has been performed to quantitively determine whether the volume of injected CO_2 remains constant or undergoes changes over time. This aspect remains relatively unexplored in the existing literature.

In this paper, we address the pressing need to quantitively investigate the long-term fate of injected CO_2 and the role of time-lapse seismic inversion techniques in this endeavor using the Sleipner field as a case study. By integrating rock physics modeling and time-lapse inversion, we aim to calculate the volume of CO_2 in place and compare it to the volume of CO_2 injected. Through a systematic analysis of our findings, we contribute to a more comprehensive understanding of the dynamics of CO_2 injection and its consequences over time. This study, grounded in practical and technical insights, seeks to bridge the knowledge gap and provide valuable guidance for future CCUS projects.

At the Sleipner field, CO_2 injection involves a method called carbon capture and storage (CCS) through subsurface injection. It starts with separating CO_2 during natural gas production, compressing it for density, and then injecting it into the Utsira formation, a deep saline aquifer. This geological reservoir's properties securely contain the CO_2. Continuous monitoring ensures its containment, marking a milestone in reducing greenhouse gas emissions and demonstrating the viability of underground CO_2 storage for climate change mitigation.

In the following sections, we present the methodology and results of our time-lapse analysis, shedding light on the critical issue of CO_2 injection's long-term impact and how we can evaluate the equivalence between the volume of injected CO_2 and the volume of CO_2 in place within the geological reservoir.

2. Background—Study Area

The Sleipner field, situated in the Norwegian sector of the North Sea (Figure 1), is the world's longest-running industrial-scale storage project [16]. Sleipner is a significant gas field operated by Equinor (formerly Statoil). It holds strategic importance as a pioneer in carbon capture and storage (CCS) projects, making it an ideal study area for investigating the effectiveness of time-lapse monitoring techniques for CO_2 storage.

The Sleipner field was discovered in 1974, and production began in 1993. It has produced around 2.9 billion barrels of oil equivalent (BOE) mainly from the Heimdal formation. The field is still active, although production levels have changed over time due to reservoir characteristics and extraction methods.

The field structure itself covers a substantial area, with various reservoirs and infrastructure. Sleipner was selected for carbon capture, utilization, and storage (CCUS) primarily due to its high CO_2 content in the produced natural gas. CO_2, being a greenhouse gas, was a concern for environmental reasons. Therefore, Sleipner became one of the first fields where CCUS was implemented to reduce CO_2 emissions.

Sequestration commenced in 1996 with an estimated injection rate of a million tons of CO_2 annually. As of 2016, 16 million tons of CO_2 have been safely stored (Table 1) [17,18].

Table 1. Showing the CO_2 accumulation per annum in the Sleipner field [18].

Year	CO_2 Accumulation (Million Tons)
1996	1
2005	8
2010	12
2015	16

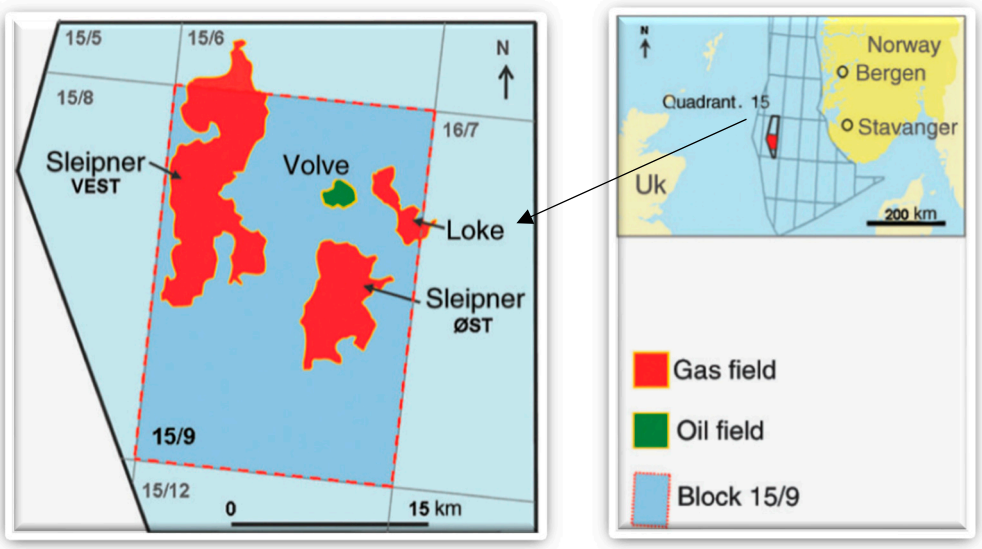

Figure 1. Map showing the Volve and Sleipner fields, Norwegian North Sea [19].

Table 1 is a plot of CO_2 accumulation (in million tons) against year. As the plot shows, about 12 million tons have been safely stored in the field as of 2010 when the latest time-lapse seismic data was acquired.

The CO_2 injection is targeted into the Utsira Formation, a regional saline aquifer (800–1000 m deep), mostly fine grained and uncemented—porosity estimates from the core range from 27% to 42%. Permeabilities are correspondingly high, with measured values ranging from 1 to 8 Darcy [20]. The caprock comprises a basin-restricted mudstone some 50 to 100 m thick. There are no known natural fractures in the reservoir.

Stratigraphically, the Utsira sand is part of the late Cenozoic post-rift succession within the North Sea Basin (Figure 2). Its eastern and western boundaries are well established through stratigraphic lap-out, while it transitions into finer-grained terrain to the southwest. Furthermore, it occupies a narrow, deepening channel to the north. The uppermost surface of the Utsira Sand exhibits varying depths, ranging from 550 to 1500 m in proximity to the Sleipner field. The base of the Utsira Sand is more intricate, featuring several mounds interpreted as mud diapirs. These mud diapirs are associated with localized faulting at the reservoir's base. However, their impact appears limited to the lower levels and does not affect the integrity of the reservoir's upper portions or the caprock [21]. The overburden above the Utsira reservoir extends about 700 m thick. The principal caprock for the reservoir is a basin-confined mudstone that extends over 50 km to the west and 40 km to the east of the Sleipner CO_2 injection area [21].

Above this mudstone caprock are sediment wedges from the late Pliocene age that consist of muddy deposits in the central basin but transition into sandier facies both in an upward direction and towards the basin margins. The shallower overburden, dating to the Quaternary age, comprises glaciomarine clays and glacial tills. This geological formation offers suitable characteristics for secure and efficient CO_2 storage [22,23].

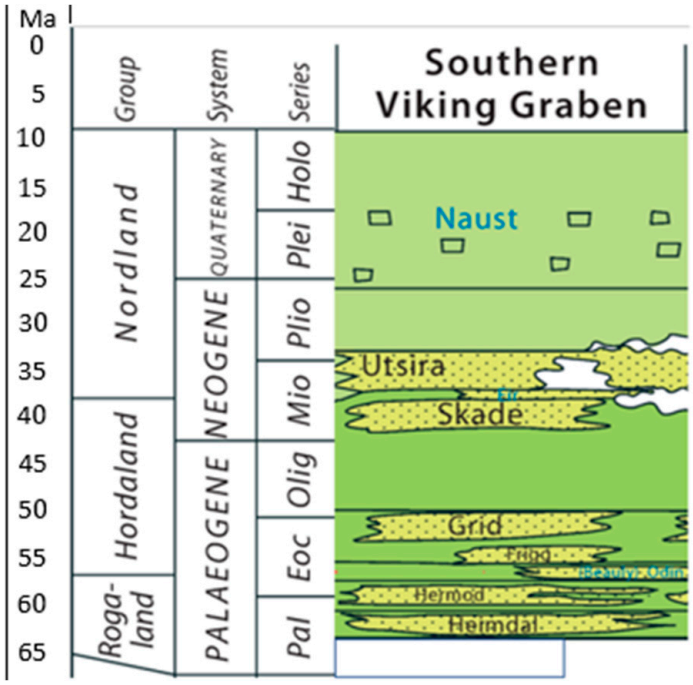

Figure 2. Chart showing the lithostratigraphic column of the North Sea showing the reservoirs of interest: Utsira Sands [23].

On well logs: mainly gamma ray log and resistivity logs, the Utsira Sand can be distinguished by its top and bottom layers, and the percentage of clean sand that makes up the reservoir unit typically exceeds 70%. The quasi-proportion comprises thin mudstones with an average thickness of approximately one meter and are expressed as peaks on the gamma-ray and resistivity logs. The "five-meter mudstone" is a thicker and more laterally persistent bed than others, and it differentiates the uppermost sand unit from the main reservoir below it. It has been demonstrated that the mudstone layers within the reservoir sand act as substantial permeability barriers, significantly influencing the amount of CO_2 that migrates through the reservoir [24].

3. CO_2 Plume Migration as Evidenced in the Monitoring 4D Seismic Data

Monitoring 4D seismic data within the Sleipner Field plays a pivotal role in gaining insights into the dynamics of the CO_2 plume's behavior within the reservoir over an extended period. To establish a reference point, an initial 3D seismic survey was conducted in 1994 before CO_2 injection commenced. This survey offered a snapshot of the reservoir's initial conditions. Importantly, this baseline data set served as a benchmark for subsequent comparisons with 4D surveys. Over CO_2 injection, periodic 3D seismic surveys were conducted at intervals of 2 to 3 years, beginning in 1996, followed by 2001 and later in 2010. The recurring surveys systematically captured the progressive evolution of the reservoir saturation, encompassing the migration of the CO_2 plume and any associated changes in reservoir pressure.

By analyzing 4D seismic data, we track our interpreted movement of the CO_2 plume within the Utsira reservoir. As CO_2 was introduced, it displaced brine and filled pore spaces, giving rise to a distinctive seismic signature. This signature was continually monitored to observe the plume's expansion and migration, as evidenced in Figures 3–5. Beyond plume dynamics, the 4D seismic data provided valuable insights into shifts in reservoir pressure. The injection of CO_2 increased reservoir pressure, manifesting as subtle variations in the reflection geometry observed in the evolving 4D seismic data.

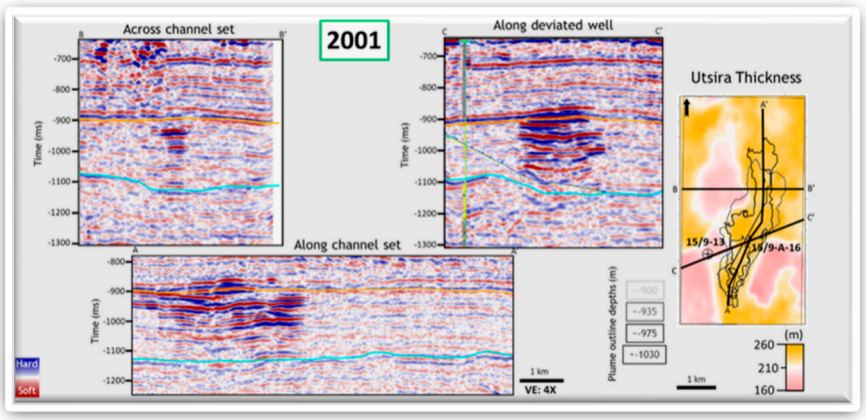

Figure 3. Seismic section in 2001 after CO_2 injection started in 1996 (Yellow corresponds to high thickness and pink corresponds to low thickness, respectively, C-C is section taken along the deviated well, B-B is section taken accrossthe channel set while A-A is section taken along the channel set).

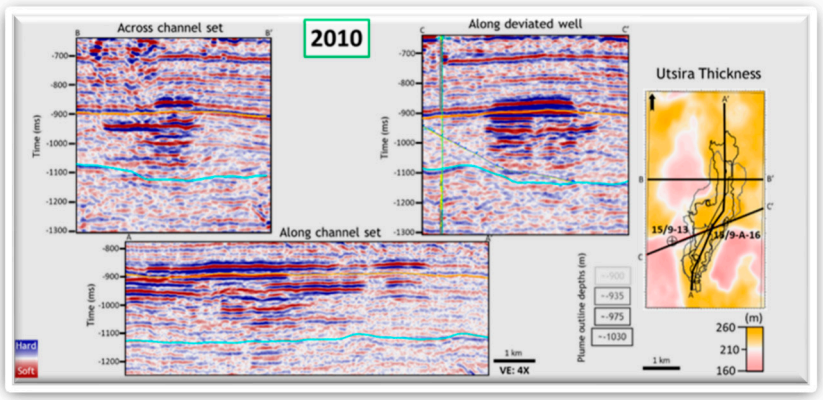

Figure 4. Seismic sections in 2010 after CO_2 injection started in 1996.

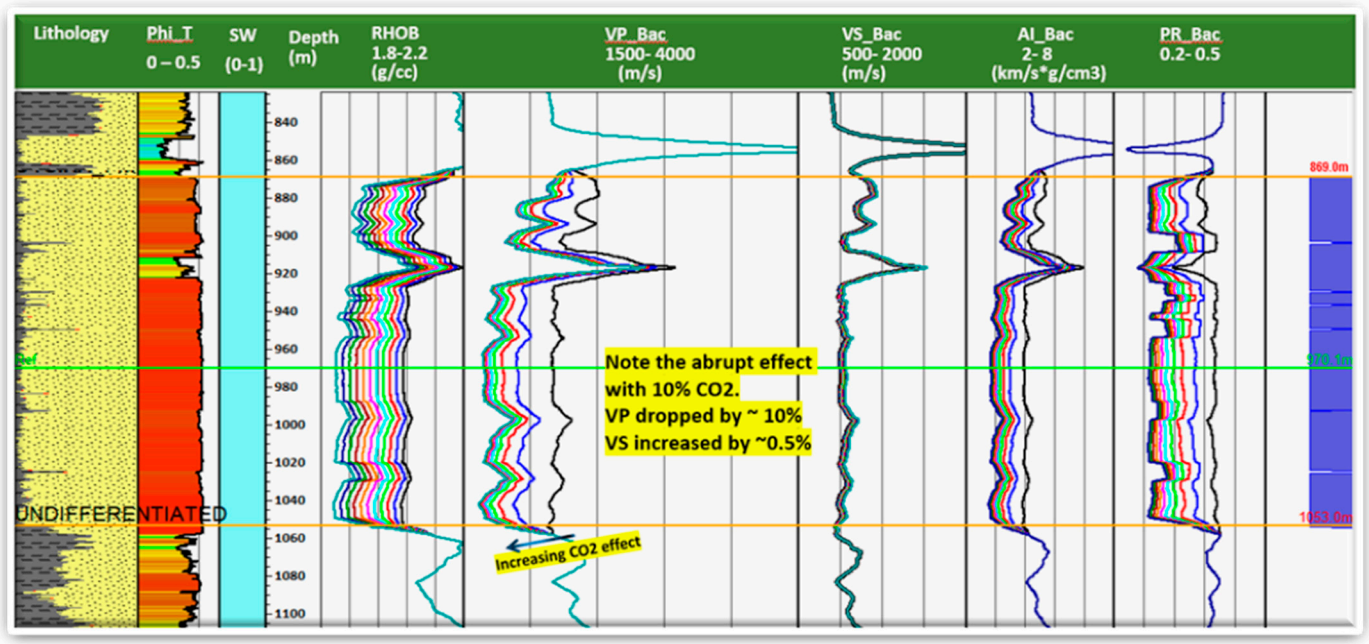

Figure 5. Fluid modeling results from left to right: lithology, porosity, saturation, depth density, V_P, V_S, AI, and PR tracks. The arrow shows a decreasing CO_2 effect.

4. Time-Lapse Synthetic Modeling

The time-lapse (4D seismic monitoring) seismic data acquired by Equinor shows the post-CO_2 injection responses in the Utsira reservoir. This elastic difference witnessed between the base and monitoring seismic data is a function of the velocity and density changes resulting from the CO_2 injection, leading to a subtle structural pull up at the top of the Utsira reservoir. Since the analysis of time-lapse seismic data involves estimating velocity and density changes resulting from the injection process, these parameters can be directly estimated from the seismic data by inverting the volume and recovering the impedance response, which is directly dependent on density and velocity. Understanding how CO_2 saturation would impart these reservoir properties requires a simplistic prior knowledge of how the CO_2 would behave in a synthetic model representative of the Utsira reservoir conditions. Therefore, we built a synthetic seismogram for the fluid modeling and performed thickness reservoir modeling to evaluate the seismic properties as a function of CO_2 saturation. The realism of the synthetic model in representing the actual reservoir conditions and fluid behavior is crucial for accurately simulating the effects of CO_2 injection on seismic properties. To ensure that the synthetic model is a direct representative of the in situ reservoir condition, the reservoir properties as seen from the well log were used and overlaid on the synthetics. Table 2 summarizes the fluid parameters used.

Table 2. Fluid properties used for synthetic modeling. For the wet reservoir condition, the density and bulk modulus of brine was assumed, and for the CO_2 reservoir condition, the density and bulk modulus of CO_2 was assumed.

Fluid	Density (Kg/m^3)	Bulk Modulus (Gpa)
Brine	1030	2.3
CO_2	0.7	0.075

With this information, new synthetics that will contain changes in velocity and density which are consistent with CO_2 flood in the reservoir were created. In Sleipner, gas has been injected into the reservoir for over 16 years and this has increased the gas saturation while displacing brine [25]. The generated synthetic represents the range of gas saturation for

different thicknesses and their responses are seen in the resultant synthetic seismic traces calculated for each scenario.

4.1. Seismic Data Conditioning

Seismic data calibration is necessary for time-lapse inversion to ensure that the data acquired at different times or under different conditions can be effectively compared and integrated to monitor the subsurface changes due to CO_2 injection over time. Seismic data are collected at different times and under varying conditions, such as changes in equipment, weather, or environmental factors. Calibration helps ensure that the data from different surveys are consistent and can be directly compared [26]. This enables trusted quantitative analysis since we aim to quantify the injected volume of CO_2. This allows for accurately interpreted and meaningful numerical values, reduced noise, and cross-validation of survey results. Here, we compare, calibrate, and analyze three 3D seismic volumes that were recorded before and after gas injection. The difference between the monitor and base was compared after each correction.

4.2. Correlation between Base and Monitor Volume

Determining the threshold parameters for the calibration process in the time-lapse inversion process, especially in estimating the volume of CO_2 injected into the Utsira Formation from seismic data, is a critical step. This process involves using cross-correlation techniques to compare the base and monitor volumes [27], particularly focusing on a data slice at the top of the Utsira Formation. Comparing the base (pre-injection) and monitor (post-injection) volumes using cross-correlation techniques quantifies the similarity in phase, frequency content, and event timing between these two datasets. The threshold we set ensures a balance between sensitivity and noise reduction, which can be a critical consideration. Fine tuning was performed through an iterative process and expert geological knowledge of the formation guided threshold selection.

Subsequently, validation of the calibration was conducted by comparing it with synthetic data, ensuring that it accurately captures significant changes while minimizing the influence of noise. This process is crucial for the accuracy of the time-lapse inversion, enabling us to effectively monitor the impact of CO_2 injection on the Utsira Formation and estimate the injected volume. It ensures that seismic data from different periods are properly aligned and calibrated, making them suitable for the quantitative analysis required in this study.

Following the cross-correlation process, the predictability between the base and monitor volumes was assessed by applying Equation (1) which determines the predictability between two volumes:

$$PRED = \frac{\sum \varnothing_{ab}(t) x \varnothing_{ab}(t)}{\sum \varnothing_{aa}(t) x \varnothing_{bb}(t)}, \quad (1)$$

where the cross-correlation operator, $\varnothing$ and the subscripts, a and b are the traces being cross correlated, and t is the time. Therefore, predictability for time t is the square of the cross correlation of the traces of the two volumes and summed up over the sample window, divided by the product of the autocorrelation of each volume also summed up over the sample window. Predictability quantifies the degree to which the values in one seismic volume align with those in the other, essentially measuring how closely the monitor data follows the base data. This analysis is vital for validating the success of the calibration process and ensuring that any variations observed between the volumes are indicative of real subsurface changes rather than artifacts or noise. By carefully examining the predictability measure, confidence was gained in the accuracy of the time-lapse inversion results and made informed interpretations about the behavior of the reservoir, whether related to CO_2 injection or other geological phenomena. Moreover, the predictability measure helped identify areas of the dataset where further calibration refinement was required.

4.3. Applying Phase and Time Matching

The phase and time matching process calibrates the time and phase shifts required to align the base and monitor datasets where injection-related effects are not anticipated. Calibration in this context involves ensuring that the seismic data from both datasets synchronize accurately [28], especially in regions where no significant changes due to CO_2 injection are expected. The phase alignment was performed iteratively, preparing the data for the quantitative analysis and change detection.

To initiate this calibration process, we begin with a first-order global phase correction and a bulk time shift. These initial shifts were applied across the entire analysis window of the monitor survey. The goal is to establish a fundamental alignment between the three datasets, ensuring that seismic events, reflections, and features are synchronized. This initial calibration step sets the foundation for further, more detailed matching processes. As the calibration progresses, additional adjustments and matching techniques can be implemented to fine-tune the alignment, considering the specific characteristics of the Utsira Formation and the intricacies of the CO_2 injection process. The iterative nature of this calibration ensures that seismic data are accurately prepared for the subsequent phases of time-lapse inversion, allowing for a more precise estimation of CO_2 injection volumes and a comprehensive understanding of the reservoir changes over time.

The phase and time matching is then performed over the entire volume and entire trace using the base volume as the reference volume with a correlation sample length of 81 targets around the Utsira formation top with a fixed window size of 400 ms. The global phase and time shift were only determined using values that were greater than the correlation threshold and lower than the shift threshold. These criteria were used with the assumption that no CO_2 injection-related data were included in the calculations. Every trace in the volume received an adjustment, but local variances are preserved.

4.4. Matching of Shaping Filter

The shaping filter process refines the alignment between the base data and the phase- and time-shifted monitor data. The primary objective is to enhance the base data, ensuring it closely matches the monitor data in terms of frequency content, phase (which can be frequency-dependent), time, and amplitude. This was achieved using the Wiener–Levinson equation [29]:

$$RF = g \tag{2}$$

where R = the autocorrelation matrix of the input

F = the desired filter

g = the cross-correlation of the desired output with the input.

The solution to this equation is then:

$$F = R^{-1}g \tag{3}$$

where R^{-1} = the matrix inverse of R.

By leveraging the shaping filter, we established a seamless and precise correspondence between the two datasets, ultimately enhancing the ability to detect and interpret subsurface changes due to CO_2 injection or other geological phenomena.

The shaping filter was designed to estimate a transfer function that effectively harmonizes the seismic characteristics of the two datasets. This includes aligning their frequency content, phase variations across different frequencies, timing of seismic events, and the overall amplitude of seismic signals. This process also involves matching the cross-correlation of the two datasets to the autocorrelation of the reference dataset, which is the base data. This intricate matching process ensures that the two datasets are aligned in terms of phase and timing and that their spectral content and overall seismic signatures closely resemble each other. The shaping filter, in conjunction with earlier calibration steps, contributes to creating a highly accurate and consistent dataset that forms the foundation for robust time-lapse inversion analysis and the estimation of CO_2 injection volumes. of the two

datasets. We match the cross correlation of the two datasets to the autocorrelation of the reference dataset (the base).

4.5. Correcting for Shallow Statics

To ensure the accuracy and reliability of our time-lapse in-version study, we focus on addressing trace-by-trace time delays caused by shallow statics—a critical step known as shallow statics correction. While the previous steps, including the shaping filter, were instrumental in aligning the seismic data in terms of their frequency content, phase, and timing, there is often an additional layer of time delays introduced by shallow subsurface factors that require correction. These shallow statics, if left unaddressed, can affect the quality of our results, particularly in regions where the gas injection has introduced timing discrepancies.

To tackle this challenge, our approach involves defining a cross-correlation window that spans from the shallow data above the zone of interest down to the topmost layer of the zone. This window captures the area where the shallow statics are most likely to have an impact. Initially, the time shift was limited to a 10-millisecond threshold, assuming that larger bulk shifts had already been corrected for in earlier calibration steps. Subsequently, time-variant statics are applied to the data after the optimized statics are implemented in the shallow data section. This multi-step process aims to bolster the correlation across all areas of interest—above, inside, and below the gas-injected region—where timing discrepancies are expected to exist. The careful correction of these shallow statics ensures that the seismic data accurately represent the subsurface changes brought about by CO_2 injection, thus enhancing the precision of our volume estimations and the overall reliability of our time-lapse inversion results.

4.6. Repicking Horizon on the Monitor Data

This process is essential for addressing challenges related to changes in subsurface velocity that occur at scales finer than the frequency content of the seismic wavelet [28]. These subtle velocity changes, often missed during the initial data acquisition, can significantly impact the inversion results. When not adequately accounted for, they can lead to inaccurate representations of reservoir changes, particularly in impedance variations. By re-picking horizons on the monitor data, we can effectively capture the time delay information. This is achieved by identifying and measuring the differences in the arrival times of seismic events between the base and monitor datasets at the selected horizon. This additional temporal information enables us to refine the inversion model below the seismic bandwidth. By doing so, we enhanced the fidelity of the inversion results, ensuring that even the subtlest subsurface changes associated with CO_2 injection are properly reflected in our impedance models. In essence, re-picking horizons is a vital component of our strategy to derive the most accurate and informative estimates of CO_2 volumes within the Utsira Formation, thereby bolstering our ability to monitor and understand the dynamic behavior of this geological system over time.

4.7. Calibration: Correcting Time-Variant Shifts, Cross-Plotting Coefficients and Shifts, and Preconditioning

In our ongoing efforts to ensure the precision of our time-lapse inversion process, we address the complex task of correcting time-variant shifts. The seismic signals' travel time through the subsurface is influenced by changes in the velocity of the reservoir below. These velocity changes can introduce temporal discrepancies in the seismic data, which we aim to correct. These adjustments are essential to isolate discrepancies related to reflectivity changes between the base and monitor surveys while filtering out structural misalignments. By applying time-variant temporal corrections, we account for variations in the velocity of the reservoir, allowing us to differentiate between the effects of CO_2 injection and other factors that may influence seismic data.

Following the correction of time-variant shifts, we move on to the cross plotting of coefficients and shifts. This step involves visualizing the cross-correlation coefficients and temporal shifts as a function of time in the seismic volumes generated during our analysis. It is important to note that the consequences of these time shifts can often appear irregular and noisy, particularly when dealing with seismic data affected by CO_2 injection. Low correlation coefficients may be observed, which are typically indicative of unsatisfactory time shifts. These low correlations can often result from the low reflectivity of certain geological features or zones within the reservoir. However, by the time the shifts are implemented in the subsequent stage, these discrepancies will be addressed and mitigated, contributing to our inversion results' overall accuracy and reliability.

In the final stage of this critical process, we focus on preconditioning the time shifts. This step serves two key objectives: firstly, it aims to limit the time shifts to the effects directly related to CO_2 injection, ensuring that fictitious, non-injection-related factors do not influence these changes. Secondly, the preconditioning process helps reduce the influence of irrelevant effects on the time shifts. It is important to emphasize that this alteration does not diminish the impact of CO_2 injection on the seismic data; rather, it refines and isolates the injection-related changes for a more precise estimation of CO_2 volumes and their associated effects within the Utsira Formation. The combination of these corrective measures strengthens the reliability and interpretability of our time-lapse inversion results, facilitating a more accurate understanding of the dynamic behavior of the geological system over time.

5. Discussion of Results

In this study, the Sleipner field data (well logs and seismic) have been investigated for petrophysical parameters prediction using rock physics modeling. The final modeled elastic curves were used to perform perturbation modeling primarily in the Utsira formation reservoir. The rock physics modeling aided in identifying the differentiation of CO_2 injection effects in the Utsira formation.

The modeling results have been summarized in Figures 5–7. Between 0 and 0.1 CO_2 saturation, there is a dramatic decrease in the acoustic responses: P-wave velocities, acoustic impedance (AI), and poisson ratio (PR). (Figure 5): with a subtle difference observed for higher saturation. In the first 10% CO_2 substitution, the P-wave velocity decrease is 12%, a subtle effect of around 1–2% is observed for higher CO_2 saturation values, and S-wave velocity (Vs) increases with CO_2 saturation. With increasing CO_2 saturation, the rock bulk modulus (Ksat) decreases. Consequently, the P-wave velocity decreases while the bulk density (b) decreases thereby decreasing the AI and PR. In contrast, the increase in S-wave velocity is directly related to CO_2 saturation. At a CO_2 saturation of 0.1%, the S-wave velocity increases subtly due to a decrease in density. Since the shear modulus remains constant and is unaffected by fluid substitution, the change in S-wave velocity depends only on bulk density variations. Figure 7 shows the synthetic seismogram results. The distinction in synthetic traces is most noticeable in the fluid substitution zone (~890–1070 m). With CO_2 increment, the amplitude changes due to the gas substitution.

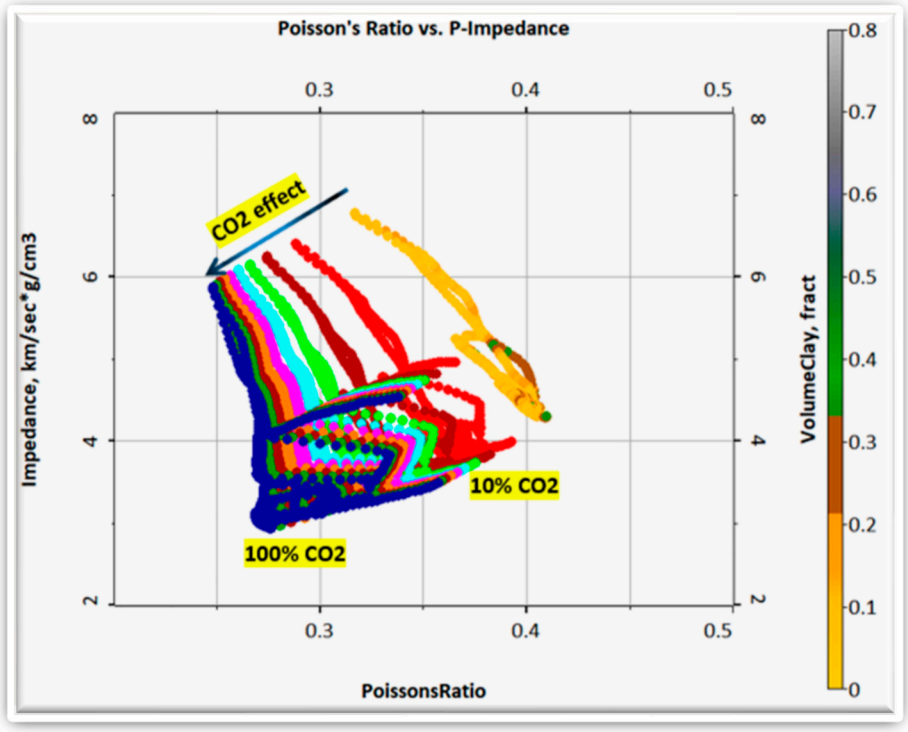

Figure 6. Cross plot of AI versus PR color-coded by V_{clay}. The arrow illustrates the decreasing CO_2 effect. The sharp effect from 0–0.2 CO_2 saturation while a more subtle effect is observed for higher CO_2 saturation values.

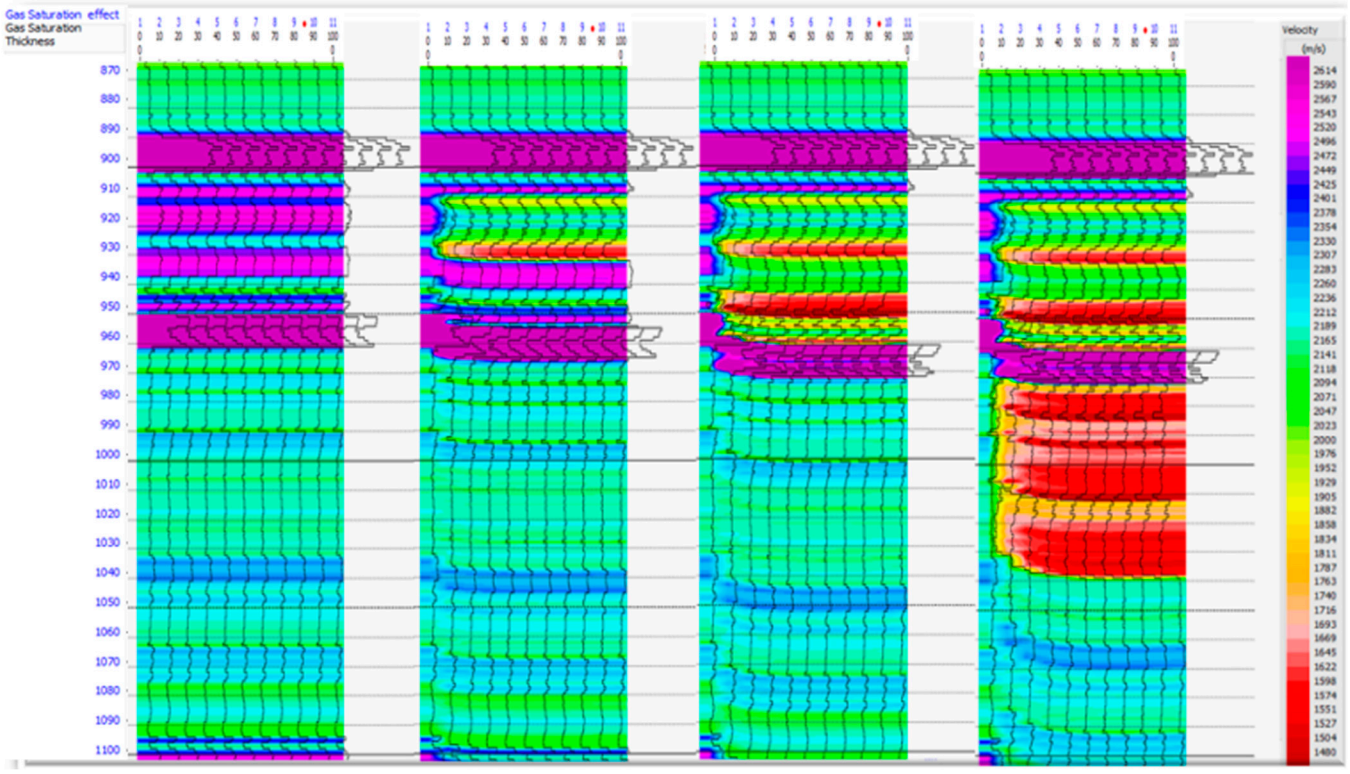

Figure 7. Shows the synthetic response of the injected CO_2 at 0%, 20%, 50%, and 100% saturations (from left to right).

5.1. Impact of Data Conditioning on Volume Estimation

Figure 8 is a cross-correlation map generated from the data calibration process, it shows a high correlation range of 60 to 100% at the data outside the CO_2 injection, while the CO_2 injection zone indicates a very low correlation of zero to 50%. This suggests a major dissimilarity between the base and monitor volume at the injection zone. This can be interpreted as the effect of the CO_2 injection on the seismic response of the monitor volume. The observed high correlation range of 60% to 100% in areas outside the CO_2 injection zone signifies a strong similarity between the base and monitor volumes in terms of phase, time, and frequency content. This indicates that the seismic signals in these regions are well aligned, suggesting that little to no subsurface changes have occurred, at least within the bandwidth of the seismic data. Conversely, the very low correlation of zero to 50% within the CO_2 injection zone suggests significant dissimilarity between the two datasets. This disparity can be attributed to the impact of CO_2 injection on the seismic response in the monitor volume, which could result from changes in subsurface properties like reservoir saturation, pressure, or fluid distribution.

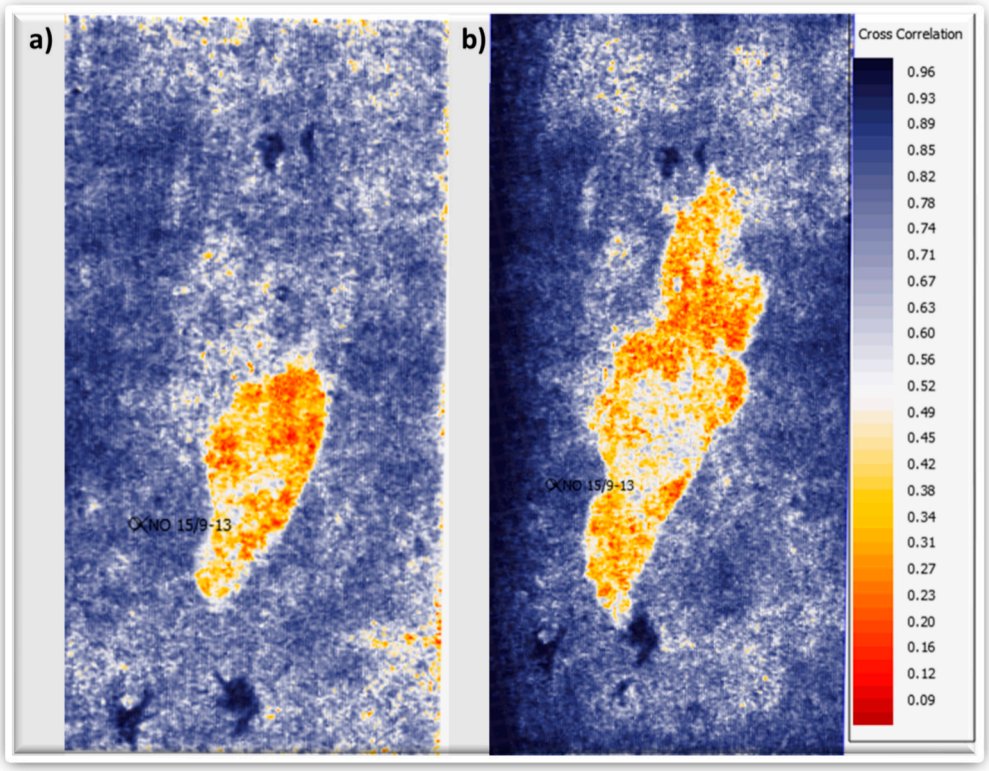

Figure 8. Cross-correlation map of the base map and the 2001 (**a**) and 2010 (**b**) monitor volumes. It shows a high correlation range of 60 to 100% at the data outside the CO_2 injection, while the CO_2 injection zone indicates a very low correlation of zero to 50%.

The lower correlation values within the CO_2 injection zone might imply a phase shift, indicating that seismic events within this region are not aligning properly with their counterparts in the base data. This could reflect changes in the subsurface, such as alterations in lithology or fluid properties caused by the injection. Additionally, time differences may suggest that seismic reflections within the CO_2-affected area arrive later in the monitor data, compared to the base data. This can be indicative of changes in reservoir properties or pressure-related effects introduced by the CO_2 injection. Frequency differences might indicate that the seismic wavelet characteristics within the injection zone have undergone alterations, possibly due to variations in the reservoir's mechanical properties or fluid distribution.

Understanding these phase, time, and frequency differences is instrumental in positive volume estimation. It provides insights into the magnitude and nature of the changes within the injection zone. By quantifying these differences, you can refine our time-lapse inversion models to accurately account for the effects of CO_2 injection. The spatial distribution of these variations can help create more detailed reservoir models and improve the accuracy of volume estimation. Additionally, the correlations and differences observed in the map can guide the selection of calibration thresholds, influence time-shift adjustments, and aid in the application of inversion techniques that consider these phase, time, and frequency variations. Ultimately, a comprehensive analysis of the cross-correlation map enhances our ability to quantify the volume of CO_2 injected and its effects on the Utsira Formation with greater precision and confidence.

The correlation analysis also resulted in an envelope map. Figure 9 shows that the value of the envelope map within the injection zone ranges from 0.31 to 0.54 while regions outside the injection area show higher envelop values ranging from 0.61 to 0.97. The envelope map provides an additional layer of information that complements the cross-correlation analysis in our ongoing discussion. The envelope map values reflect the magnitude or strength of the seismic signal at each location within the dataset. In the context of time-lapse inversion for CO_2 injection monitoring, the variation in envelope values within and outside the injection zone is particularly insightful. The lower envelope values within the injection area (ranging from 0.31 to 0.54) suggest a weaker seismic signal response. This could be indicative of reduced reflectivity, perhaps caused by changes in reservoir properties or fluid content associated with the CO_2 injection. In contrast, regions outside the injection area exhibiting higher envelope values (ranging from 0.61 to 0.97) suggest stronger seismic responses, reflecting relatively stable subsurface conditions.

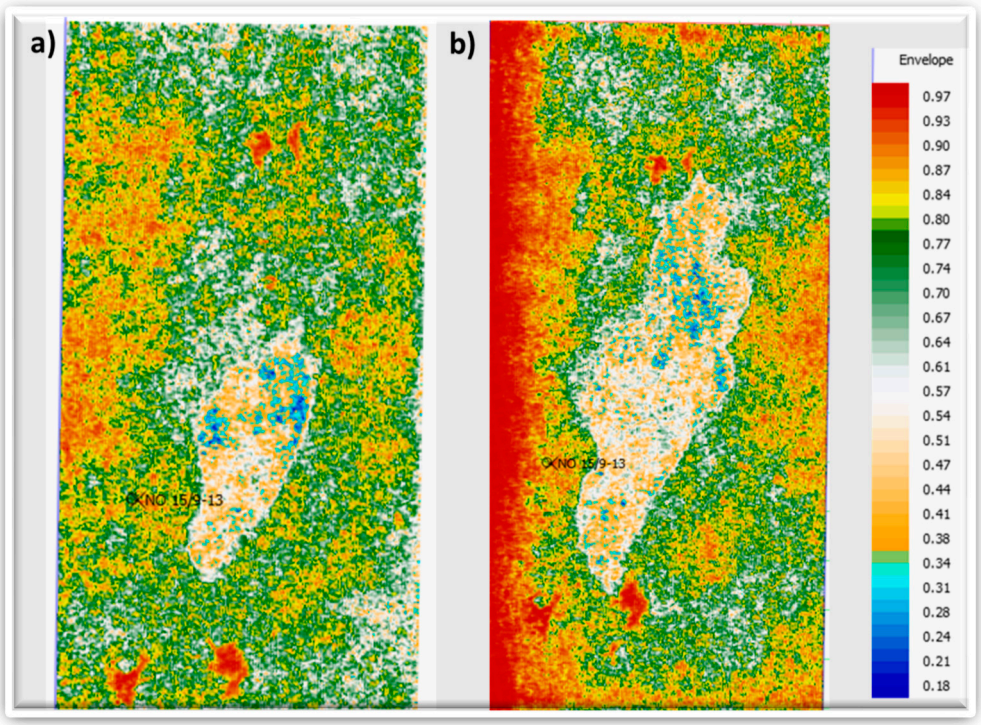

Figure 9. Envelope map of the 2001 (**a**) and 2010 (**b**) monitor volumes. The value of the envelope within the injection zone ranges from 0.31 to 0.54 while regions outside the injection area show higher envelope values ranging from 0.61 to 0.97.

Comparing the envelope map to the cross-correlation map, it becomes apparent that these two datasets provide complementary information. While the cross-correlation map focuses on the alignment and similarity of seismic waveforms, the envelope map

emphasizes the strength or amplitude of the seismic signals. The envelope values can vary due to changes in reflectivity, fluid saturation, or mechanical properties within the reservoir. In the context of volume estimation, this information is valuable because it allows you to identify areas where the seismic response has been significantly affected by CO_2 injection. The lower envelope values within the injection zone provide quantitative evidence of the changes in subsurface properties, which can be directly incorporated into our time-lapse inversion models. This aids in refining the accuracy of volume estimation by directly linking the strength of the seismic signal to subsurface changes, thereby enhancing the reliability and precision of our estimates of injected CO_2 volumes and their effects on the Utsira Formation. It also provides a more complete picture of how the CO_2 injection has influenced the seismic data, going beyond just phase and time shifts, and enabling a more comprehensive understanding of the dynamic behavior of the subsurface over time.

The predictability map (Figure 10) quantifies how predictable the traces within the injection zone are compared to those outside the injection zone, taking into account the base volume. The low predictability within the injection zone, ranging from 0 to 0.34, indicates that the seismic responses within this area are less predictable when compared to those outside the injection zone, which exhibit predictability values ranging from 0.45 to 0.96. This disparity reinforces the understanding that the seismic data within the injection zone are less consistent and exhibit a higher degree of variability compared to areas unaffected by CO_2 injection.

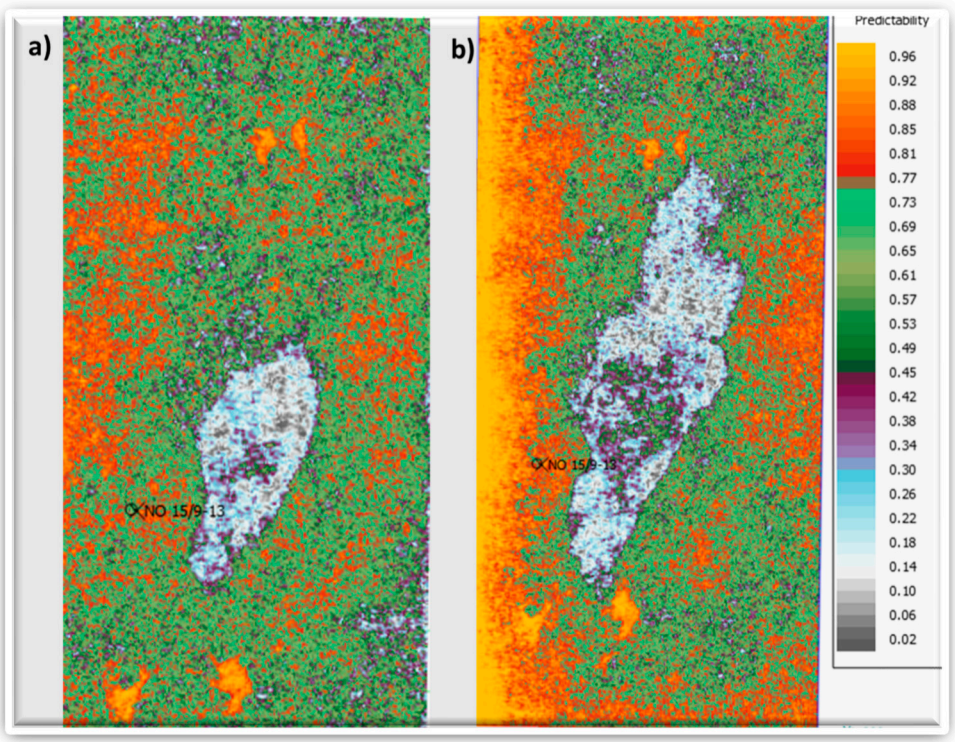

Figure 10. Computed predictability map of the (**a**) 2001 and (**b**) 2010 monitor volumes. The low predictability within the injection zone, ranges from 0 to 0.34, indicates that the seismic responses within this area are less predictable when compared to those outside the injection zone, which exhibit predictability values ranging from 0.45 to 0.96.

The low predictability within the injection zone correlates with the low envelope values, suggesting weaker seismic responses and less consistent seismic patterns within this region. Additionally, it aligns with the low correlation values observed in the cross-correlation map, indicating that seismic waveforms within the injection zone are less aligned with their counterparts in the base data. Together, these findings underscore the complex and dynamic nature of the seismic response within the injection zone, which can

be attributed to the effects of CO_2 injection. This integrated understanding of predictability, envelope, and cross-correlation results is instrumental in refining the accuracy of volume estimation and enhancing our ability to monitor and interpret the subsurface changes associated with CO_2 injection within the Utsira Formation.

The phase map generated (Figure 11) presents an important perspective on the seismic response in both the injection and non-injection zones, and it complements the earlier findings in our ongoing discussion. The observed phase values ranging from −43.20 to 43.20 degrees at the non-injection zones suggest a relatively uniform and consistent phase behavior within these areas. This consistency indicates that seismic waveforms in the non-injection zones maintain a coherent alignment and phase relationship between the base and monitor surveys. The low variation in phase values suggests minimal changes in subsurface properties or fluid distribution within these regions.

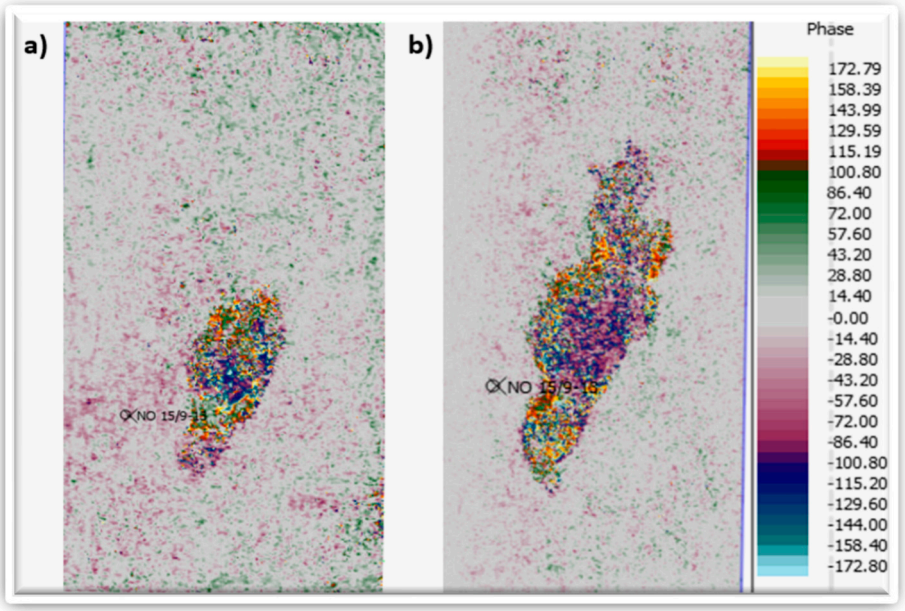

Figure 11. Computed phase map for the (**a**) 2001 and (**b**) 2010 monitor volumes. The observed phase values range from −43.20 to 43.20 degrees at the non-injection zones suggesting a relatively uniform and consistent phase behavior within these areas. The phase values within the injection zone exhibit a wider range, varying between 57.60 to 172 degrees and −57.60 to −172 degrees.

In contrast, the phase values within the injection zone exhibit a wider range, varying between 57.60 to 172 degrees and −57.60 to −172 degrees. This wide range of phase values signifies a more complex and variable phase behavior in response to CO_2 injection. The positive and negative phase values can be attributed to phase shifts introduced by changes in subsurface properties, fluid content, or reservoir pressure associated with the injection. The greater phase variations in the injection zone are reflective of the dynamic alterations introduced by CO_2 injection activities. These phase changes provide critical information for understanding the impact of CO_2 injections on the seismic response, particularly within the Utsira Formation.

The final normalized difference amplitude map (Figure 12) reveals a significant reduction in differences to about 50% of the original signal level in areas unaffected by injection, which is a testament to the effectiveness of the 4D time-lapse inversion process. This outcome reflects the intricate and systematic steps taken to align and compare the base and monitor seismic data over time. By systematically applying these techniques and insights, the 4D time-lapse inversion process optimizes the seismic data for areas unaffected by injection, reducing the original signal differences to about 20% of their initial levels. This reduction in disparities ensures that the seismic data more accurately represent subsurface changes, enabling a more precise estimation of CO_2 volumes and enhancing

our understanding of reservoir behavior over time. The successful reduction of differences is indicative of the process's ability to effectively capture and account for the dynamic variations introduced by CO_2 injection, ultimately strengthening the reliability of the inversion results.

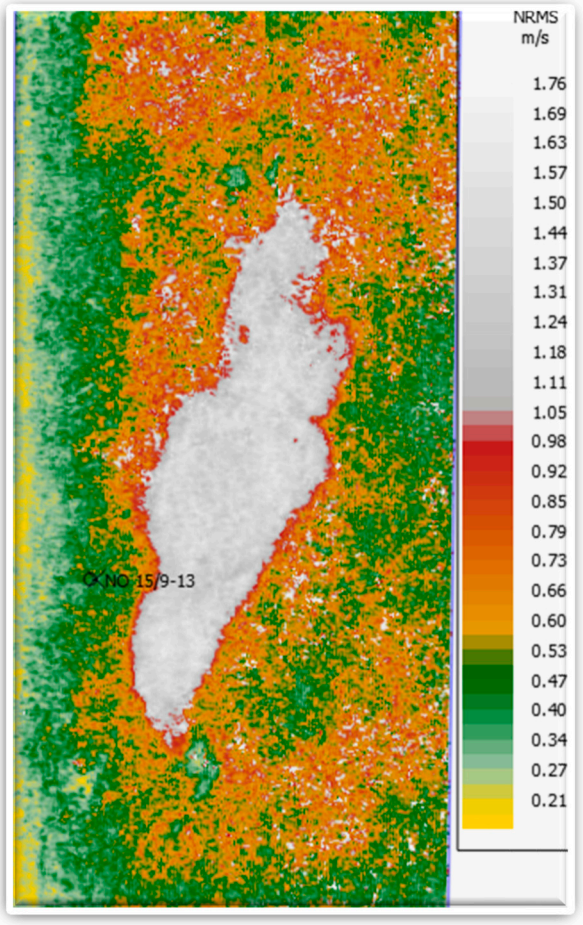

Figure 12. Root-mean-square amplitude showing the final base monitor difference. The white-colored region shows the CO_2 plume extent within the injection zone, while the rest colors show the background.

In the context of our ongoing discussion, the phase map complements the findings from the predictability, envelope, and cross-correlation analyses [30]. It confirms that the seismic response within the injection zone is indeed more complex and dynamic, with noticeable phase variations that may be linked to CO_2-induced changes in the subsurface [31]. These phase changes contribute to the overall understanding of how CO_2 injections influence seismic data and are invaluable for refining time-lapse inversion models [32]. By integrating this phase information, we can obtain a more detailed and precise characterization of the changes introduced by CO_2 injections within the Utsira Formation [15]. This holistic approach strengthens the accuracy of volume estimation and enhances our ability to monitor and interpret the evolving behavior of the reservoir over time [33].

Maintaining the observed difference in impedances (as shown in Figure 13) between the injection and non-injection zones within the predictability map is a deliberate choice made to ensure that the effects of CO_2 injections are accurately and precisely quantified during the time-lapse inversion process. By allowing this disparity to persist, we retain a direct representation of the distinct seismic responses within the injection zone, explicitly linked to the presence and impact of CO_2 injections. This differentiation is essential for isolating and quantifying the changes introduced by injection activities, including modifications in reservoir properties and variations in fluid distribution.

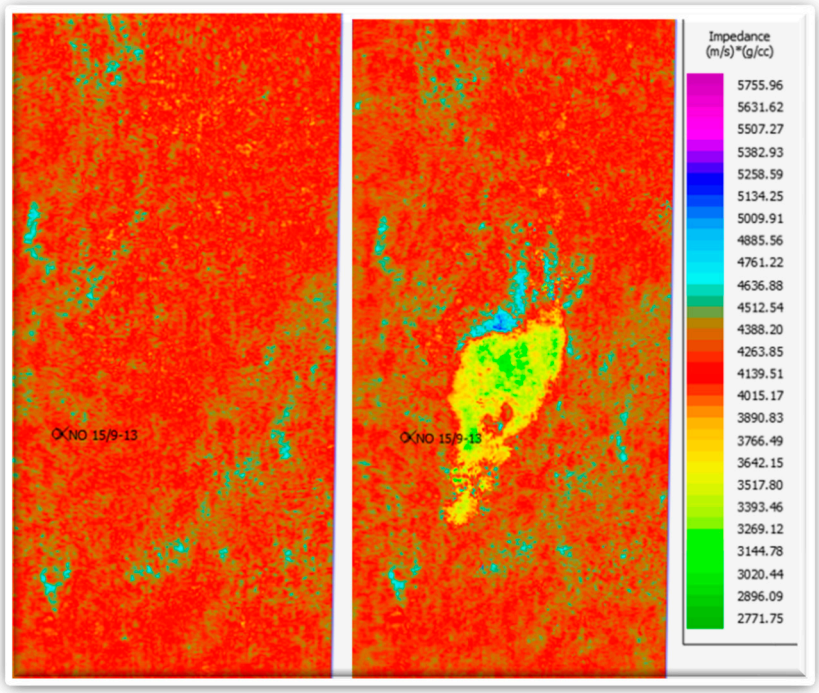

a) **b)**

Figure 13. Inverted base (**a-left**) and monitor (**b-right**) seismic volume for Utsira formation showing the impedance contrast between the background and injection zone.

In essence, the deliberate preservation of this disparity serves as a strategic decision to distinguish between the dynamically changing injection zone and the comparatively stable non-injection zone. This strategy enables a more focused and accurate characterization of the effects of CO_2 injections, such as shifts in reservoir saturation, pressure, or fluid properties. These disparities provide a clear contrast between areas that have experienced substantial changes due to injections and those that have maintained relative stability. Consequently, this approach enhances the reliability of the time-lapse inversion process, facilitating a more precise estimation of CO_2 volumes and their influence on the Utsira Formation. This, in turn, supports well-informed decision making in reservoir management and environmental assessment.

5.2. Enhanced Inversion and CO_2 Volume Estimation

It is imperative to highlight the significance of inverting seismic time-lapse volumes, as it yields crucial insights into acoustic impedance changes between the base and monitor surveys. However, the process is not without its challenges, notably the time delays introduced by reservoir velocity changes that can impact the accuracy of inversion comparisons. These velocity changes often operate below the frequency content of the seismic wavelet, rendering the impedance or velocity differences less effective in accurately representing reservoir variations. To address this, we have integrated time delay information into our inversion approach, enhancing the process and capturing valuable information beyond the seismic bandwidth.

In our study, we leveraged cross-correlation and time-shift cubes to calculate velocity decreases, offering an effective means to determine time-variant statistics. We then applied these insights by multiplying scalers with initial models to extract low-frequency information. This strategic approach has yielded significant improvements in the inversion process, allowing us to capture subtler variations within the reservoir. By incorporating time delay information and low-frequency data, our inversion models can more accurately depict the changes brought about by CO_2 injection, thus enhancing the precision and reliability of our

volume estimations and overall understanding of the dynamic behavior within the Utsira Formation.

The inversion result displayed in Figure 13 for both the base (a) and monitor (b) data provides a clear and insightful depiction of the effects of CO_2 injection within the Utsira Formation. As anticipated, the injection zone prominently stands out, characterized by a notably lower impedance range spanning from approximately 2700 to 3800 m/sg/cc. In contrast, the background impedance values range from approximately 3900 to 5000 m/sg/cc. This stark contrast in impedance values between the injection and background zones effectively delineates the region influenced by the injected CO_2. The distinct and lower impedance values in the injection zone are a direct consequence of changes in reservoir properties, such as alterations in fluid distribution and saturation, attributed to the CO_2 injection. In Figure 13b, the monitor data's representation of the CO_2 plumes provides valuable insights into the extent and behavior of the injected CO_2. Notably, the impedance values around the non-injection zone remain relatively stable, exhibiting minimal variation. This stability in impedance within the non-injection zone serves as a key reference point for outlining the extent of the CO_2 plumes. The distinctiveness of the plume outline is indicative of the effectiveness of the inversion process in capturing the CO_2-induced changes in impedance. This result reinforces the accuracy of the plume delineation, allowing for a precise representation of the CO_2 distribution within the Utsira Formation. The combination of these inversion outcomes significantly contributes to the reliable estimation of CO_2 volumes and an enhanced understanding of CO_2 migration and behavior within the subsurface reservoir. Notice that the northernmost part of the injection zone (black arrow) shows an anomalously high impedance compared to rest of the background. This is probably due to facies change inhibiting the CO_2 migration towards the northwest direction. These facies appear to have a separate response from the rest of the background, allowing it to be categorized as an anomalous CO_2 response in our previous analysis. It can also be a result of an edge artifact resulting from processing velocity.

While it is essential to acknowledge the non-uniqueness inherent in the inversion result [34], we pursued a systematic approach to estimate the volumetric changes evident in the 4D anomaly map, reflecting seismic variations attributed to the injection process. To enhance the precision of our time-lapse interpretation, we calculated the reservoir volume affected by the injection process and then cross referenced it with the recorded injection volumes for the field. This cross referencing served to mitigate the inherent non-uniqueness in time-lapse analysis. The volumetric area was derived from the inversion volume as shown in Figure 14. The figure shows a 3-dimensional perspective of the plume area and thickness, and this agrees with our knowledge of its geological characteristics, which was interpreted to be a channel complex [35].

To refine our volumetric analysis, we used an average porosity of 38%, which was estimated from well logs. In Sleipner, where CO_2 injection into the Utsira formation spanned from 1996 until 2010, the gas tank's depth was assumed to fall within the range of 250 to 300 m, based on contact logging. With these parameters in place, we assumed a formation volume factor (FVF) of 1.2 and generated multiple realizations, as detailed in Table 3. To isolate the specific cells corresponding to time-lapse changes, we identified zones on the inversion map and established a threshold. This rigorous approach allowed us to more accurately estimate the volume of injected CO_2, contributing to a refined understanding of the injection's effects within the Utsira Formation. As shown in Table 3, the calculated volume is very close to the actual volume of the injected CO_2, with a calculated—actual (C/A) ratio range of 0.9 to 1.1, assuming that 12 million tons of CO_2 had been injected by 2010. This is an improvement over previous estimations which have wider differences.

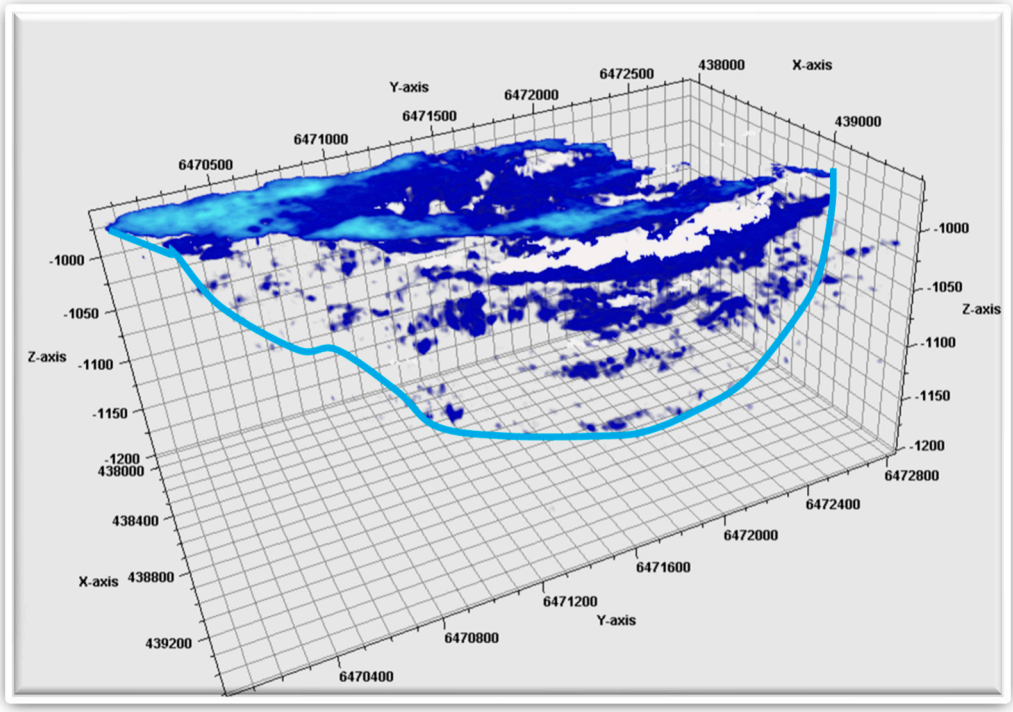

Figure 14. 3D perspective of the injected CO_2 volume and extent of the plume migrations. The CO_2 fit into the channel discussed in the introduction.

Table 3. CO_2 volume estimation using the calculated volume-to-actual volume ratio.

	Calculated Volume (m^3)	Actual Volume (m^3)	C/A Ratio
1	3.78×10^7	3.40×10^7	1.1128
2	3.49×10^7	3.40×10^7	1.0282
3	3.88×10^7	3.40×10^7	1.1414
4	3.57×10^7	3.40×10^7	1.0512
5	3.35×10^7	3.40×10^7	0.9850
6	4.11×10^7	3.40×10^7	1.2100
7	3.88×10^7	3.40×10^7	1.1410
8	3.37×10^7	3.40×10^7	0.9930
9	3.54×10^7	3.40×10^7	1.0420
10	3.44×10^7	3.40×10^7	1.0110
11	3.37×10^7	3.40×10^7	0.9910
12	3.81×10^7	3.40×10^7	1.1210
13	3.48×10^7	3.40×10^7	1.0230
14	3.06×10^7	3.40×10^7	0.9000
15	3.53×10^7	3.40×10^7	1.0400

6. Conclusions

Several volume estimation approaches have been adopted for monitoring CO_2 injection in the Sleipner Field. One common method involves reservoir simulation, which employs numerical models to simulate the behavior of CO_2 within the subsurface reservoir. While this approach offers valuable insights, it relies on numerous assumptions about reservoir properties and fluid behavior, which can introduce uncertainty. Additionally,

traditional seismic monitoring approaches that use differences in acoustic impedance for volume estimation may struggle to accurately capture subtle changes in the reservoir due to CO_2 injection, particularly if these changes are below the seismic bandwidth. Such methods might not fully utilize the additional information available in 4D seismic data, including phase, time, and frequency shifts, which our approach leverages.

Our approach to enhancing the time-lapse inversion method stands out for several reasons. It effectively integrates 4D seismic data with a range of advanced analyses, including cross correlation, envelope, predictability, and phase and time shifts, to comprehensively capture changes within the reservoir due to CO_2 injection. This approach provides a holistic view of the subsurface dynamics and directly links seismic data with reservoir properties. By combining multiple data facets and leveraging knowledge of the seismic wavelet's frequency content, we can more accurately estimate CO_2 volumes and assess their impact. This method reduces the non-uniqueness often associated with inversion and enhances the accuracy of volume estimations. Overall, our approach excels in its ability to capture subtle, dynamic reservoir changes brought about by CO_2 injection, offering superior insights into the behavior of the CO_2 plume in the Sleipner Field. This approach can be globally employed for estimating injected CO_2 and ensuring they are not leaking. It offers a great opportunity for the energy industry to effectively monitor injected volume and be able to account for it in the long run.

Author Contributions: Conceptualization, D.P.-D.; methodology, D.P.-D. and B.O.N.; software, D.P.-D. and B.O.N.; validation, R.R.S.; formal analysis, D.P.-D.; investigation, R.R.S.; resources, D.P.-D. and R.R.S.; data curation, D.P.-D. and B.O.N.; writing—original draft preparation, B.O.N. and D.P.-D.; writing—review and editing, D.P.-D. and B.O.N.; visualization, D.P.-D.; supervision, R.R.S.; project administration, D.P.-D. and R.R.S.; and funding acquisition, R.R.S. All authors have read and agreed to the published version of the manuscript.

Funding: This research was funded by Subsea Systems Institute and Allied Geophysics Laboratory (AGL) at the University of Houston.

Institutional Review Board Statement: Not applicable.

Informed Consent Statement: Not applicable.

Data Availability Statement: Data are contained within the article.

Acknowledgments: We also wish to express our gratitude to Subsea Systems Institute and Allied Geophysics Laboratory (AGL) for supporting this research, Equinor for providing the data, PGS and CGG for providing the software and William Marin for their support.

Conflicts of Interest: The authors declare no conflict of interest.

References

1. Wang, F.; Harindintwali, J.D.; Yuan, Z.; Wang, M.; Wang, F.; Li, S.; Yin, Z.; Huang, L.; Fu, Y.; Li, L.; et al. Technologies and perspectives for achieving carbon neutrality. *Innovation* **2021**, *2*, 100180. [CrossRef] [PubMed]
2. Zhang, Z.; Wang, T.; Blunt, M.J.; Anthony, E.J.; Park, A.H.A.; Hughes, R.W.; Yan, J. Advances in carbon capture, utilization and storage. *Appl. Energy* **2020**, *278*, 115627. [CrossRef]
3. Rutqvist, J. The geomechanics of CO_2 storage in deep sedimentary formations. *Geotech. Geol. Eng.* **2012**, *30*, 525–551. [CrossRef]
4. Hajiabadi, S.H.; Bedrikovetsky, P.; Borazjani, S.; Mahani, H. Well Injectivity during CO_2 geosequestration: A review of hydro-physical, chemical, and geomechanical effects. *Energy Fuels* **2021**, *35*, 9240–9267. [CrossRef]
5. Satoh, H.; Shimoda, S.; Yamaguchi, K.; Kato, H.; Yamashita, Y.; Miyashiro, K.; Saito, S. The long-term corrosion behavior of abandoned wells under CO_2 geological storage conditions:(1) Experimental results for cement alteration. *Energy Procedia* **2013**, *37*, 5781–5792. [CrossRef]
6. Benisch, K.; Bauer, S. Short-and long-term regional pressure build-up during CO_2 injection and its applicability for site monitoring. *Int. J. Greenh. Gas Control* **2013**, *19*, 220–233. [CrossRef]
7. Benson, S.; Myer, L. Monitoring to ensure safe and effective geologic sequestration of carbon dioxide. In Proceedings of the Workshop on Carbon Dioxide Capture and Storage, Regina, SK, Canada, 18–21 November 2002.

8. Shao, Q.; Boon, M.; Youssef, A.; Kurtev, K.; Benson, S.M.; Matthai, S.K. Modelling CO_2 plume spreading in highly heterogeneous rocks with anisotropic, rate-dependent saturation functions: A field-data based numeric simulation study of Otway. *Int. J. Greenh. Gas Control* **2022**, *119*, 103699. [CrossRef]
9. Soltanian, M.R.; Amooie, M.A.; Cole, D.R.; Graham, D.E.; Hosseini, S.A.; Hovorka, S.; Moortgat, J. Simulating the Cranfield geological carbon sequestration project with high-resolution static models and an accurate equation of state. *Int. J. Greenh. Gas Control* **2006**, *54*, 282–296. [CrossRef]
10. Huang, C.; Zhu, T. Towards real-time monitoring: Data assimilated time-lapse full waveform inversion for seismic velocity and uncertainty estimation. *Geophys. J. Int.* **2022**, *223*, 811–824. [CrossRef]
11. Souza, R.; Lumley, D.; Shragge, J.; Davolio, A.; Schiozer, D.J. Analysis of time-lapse seismic and production data for reservoir model classification and assessment. *J. Geophys. Eng.* **2018**, *15*, 1561–1587. [CrossRef]
12. Hetz, G.; Datta-Gupta, A. Integration of Time-Lapse Seismic and Production Data: Analysis of Spatial Resolution. *Transp. Porous Media* **2020**, *134*, 679–705. [CrossRef]
13. Arts, R.J.; Elsayed, R.; Van Der Meer, L.; Eiken, O.; Ostmo, S.; Chadwick, A.; Zinszner, B. Estimation of the mass of injected CO_2 at Sleipner using time-lapse seismic data. In Proceedings of the 64th European Association of Geoscientists & Engineers (EAGE) Conference and Exhibition, Florence, Italy, 27 May 2002. [CrossRef]
14. Ghaderi, A.; Landrø, M. Estimation of thickness and velocity changes of injected carbon dioxide layers from prestack time-lapse seismic data. *Geophysics* **2009**, *74*, O17–O28. [CrossRef]
15. Chadwick, R.A.; Marchant, B.P.; Williams, G.A. CO_2 storage monitoring: Leakage detection and measurement in subsurface volumes from 3D seismic data at Sleipner. *Energy Procedia* **2014**, *63*, 4224–4239. [CrossRef]
16. Cowton, L.R.; Neufeld, J.A.; White, N.J.; Bickle, M.J.; Williams, G.A.; White, J.C.; Chadwick, R.A. Benchmarking of vertically-integrated CO_2 flow simulations at the Sleipner Field, North Sea. *Earth Planet. Sci. Lett.* **2018**, *491*, 121–133. [CrossRef]
17. Furre, A.K.; Eiken, O.; Alnes, H.; Vevatne, J.N.; Kiær, A.F. 20 years of monitoring CO_2 injection at Sleipner. *Energy Procedia* **2017**, *114*, 3916–3926. [CrossRef]
18. Chadwick, R.A.; Kirby, G.A.; Holloway, S.; Gregersen, U.; Johannessen, P.N.; Zweigel, P.; Arts, R. *Saline Aquifer CO_2 Storage (SACS2)*; Final Report, Geological Characterization of the Utsira Sand Reservoir and Caprocks (Work Area 1); British Geological Survey: Nottingham, UK, 2002; 79p. Available online: https://nora.nerc.ac.uk/id/eprint/511461/ (accessed on 22 September 2023).
19. Ravasi, M.; Vasconcelos, I.; Curtis, A.; Kritski, A. Vector-acoustic reverse time migration of Volve ocean-bottom cable data set without up/down decomposed wavefields. *Geophysics* **2015**, *80*, S137–S150. [CrossRef]
20. Dupuy, B.; Romdhane, A.; Eliasson, P.; Querendez, E.; Yan, H.; Torres, V.A.; Ghaderi, A. Quantitative seismic characterization of CO_2 at the Sleipner storage site, North Sea. *Interpretation* **2017**, *5*, SS23–SS42. [CrossRef]
21. Zweigel, P.; Arts, R.; Lothe, A.E.; Lindeberg, E.B. Reservoir geology of the Utsira Formation at the first industrial-scale underground CO_2 storage site (Sleipner area, North Sea). *Geol. Soc. Lond. Spec. Publ.* **2004**, *233*, 165–180. [CrossRef]
22. Olsen, L.; Sveian, H.; Ottesen, D.; Rise, L. Quaternary glacial, interglacial and interstadial deposits of Norway and adjacent onshore and offshore areas. *Quat. Geol. Nor. Geol. Surv. Nor. Spec. Publ.* **2013**, *13*, 79–144. Available online: https://www.ngu.no/upload/Publikasjoner/Special%2520publication/SP13_s79-144.pdf (accessed on 4 October 2023).
23. Norwegian Petroleum, (2015, February 24). Field: Volve. Norwegianpetroleum. No. Available online: https://www.norskpetroleum.no/en/facts/field/volve/ (accessed on 11 October 2021).
24. Arts, R.J.; Chadwick, A.; Eiken, O.; Thibeau, S.; Nooner, S. Ten years' experience of monitoring CO_2 injection in the Utsira Sand at Sleipner, offshore Norway. *First Break* **2008**, *26*. [CrossRef]
25. Cho, Y.; Jun, H. Estimation and uncertainty analysis of the CO_2 storage volume in the Sleipner field via 4D reversible-jump Markov-chain Monte Carlo. *J. Pet. Sci. Eng.* **2021**, *200*, 108333. [CrossRef]
26. Romdhane, A.; Dupuy, B.; Querendez, E.; Eliasson, P. Toward quantitative CO_2 monitoring at Sleipner, Norway. *Geophys. Monit. Geol. Carbon Storage* **2022**, 383–402. [CrossRef]
27. Wang, Y.; Morozov, I. Waveform Calibration of Time-Lapse Seismic Data, Geoconvention, Calgary, Canada, 7–11 May 2018. Available online: https://geoconvention.com/wp-content/uploads/abstracts/2018/204_GC2018_Waveform_Calibration_of_Time-Lapse_Seismic_Data.pdf (accessed on 12 October 2023).
28. Levson, N. The Wiener (root mean square) error criterion in filter design and prediction. *J. Math. Phys.* **1946**, *25*, 261–278. [CrossRef]
29. Hanafy, S.M.; Hoteit, H.; Li, J.; Schuster, G.T. Near-surface real-time seismic imaging using parsimonious interferometry. *Sci. Rep.* **2021**, *11*, 7194. [CrossRef]
30. Arts, R.; Eiken, O.; Chadwick, R.A.; Zweigel, P.; Van der Meer, L.; Zinszner, B. Monitoring of CO_2 injected at Sleipner using time-lapse seismic data. *Energy* **2004**, *29*, 1383–1393. [CrossRef]
31. Nooner, S.L.; Zumberge, M.A.; Eiken, O.; Stenvold, T. Constraints on in situ density of CO_2 within the Utsira formation from time-lapse seafloor gravity measurements. *Int. J. Greenh. Gas Control* **2007**, *1*, 198–214. [CrossRef]
32. Arts, R.; Eiken, O.; Chadwick, A.; Zweigel, P.; Van Der Meer, B.; Kirby, G. Seismic monitoring at the Sleipner underground CO_2 storage site (North Sea). *Geol. Soc. Lond. Spec. Publ.* **2004**, *233*, 181–191. [CrossRef]

33. Sasagawa, G.S.; Crawford, W.; Eiken, O.; Nooner, S.; Stenvold, T.; Zumberge, M.A. A new sea-floor gravimeter. *Geophysics* **2003**, *68*, 544–553. [CrossRef]
34. Nwafor, B.O.; Hermana, M.; Elsaadany, M. Geostatistical Inversion of Spectrally Broadened Seismic Data for Re-Evaluation of Oil Reservoir Continuity in Inas Field, Offshore Malay Basin. *J. Mar. Sci. Eng.* **2022**, *10*, 727. [CrossRef]
35. Nwafor, B.O.; Hermana, M. Harmonic Extrapolation of Seismic Reflectivity Spectrum for Resolution Enhancement: An Insight from Inas Field, Offshore Malay Basin. *Appl. Sci.* **2022**, *12*, 5453. [CrossRef]